A Monte-Carlo Approach for Tracking Mobile Personnel

Milind Borkar [1], Volkan Cevher[2] and James H. McClellan[3]
[1,3]School of Electrical and Computer Engineering
Georgia Institute of Technology
777 Atlantic Drive
Atlanta, GA 30332-0250, USA
[2]Center for Automation Research
University of Maryland,
College Park, MD 20742, USA
[1]mb265@mail.gatech.edu, [2]volkan@cfar.umd.edu, [3]jim.mcclellan@ece.gatech.edu

Abstract— In this paper, we propose a Monte-Carlo method based on the particle filter framework to track footfall locations generated by mobile personnel using seismic arrays. While the particle proposal function follows a simple bootstrap approach, the novelty in our algorithm comes from a unique weighting strategy that takes into account the sparse nature of the seismic footfall signal and is robust against missed detections and clutter which could appear in the form of other impulsive sources or other walkers. Our weighting strategy automatically makes use of the wavefront shape, either planar or circular, and assigns weights in x-y space. Data association is built into the system, eliminating the need to explicitly associate the received footfall impulses with different walkers. Hence our algorithm is ideal for tracking multiple mobile personnel. We also demonstrate the fusion of our system with range information available by means of radar. Fusion with radar improves x-y tracking when range resolution is lost due to a large distance between the target and the seismic array leading to planar wavefronts.

Table of Contents

1. Introduction

Tracking walking humans based on estimated footfall locations is a problem that has been investigated in the past with limited success. Since footfalls generate seismic signals, geophone arrays are commonly used to produce measurements. Footfalls signals are impulsive and sparse in nature, and hence common narrowband beamforming techniques can not be used to estimate the source location. Most time domain approaches focus on determining the time difference of arrival (TDOA) of the footfall impulses at the array elements and use geometry to estimate the source location [1]. These methods, though simple in principle, can fail when multiple walkers are present since explicit data association is required.

We propose a Monte-Carlo method based on the particle filter framework to track footfall locations generated by mobile personnel using seismic sensor arrays. While the particle proposal function follows a simple bootstrap approach, the novelty in our algorithm comes from a unique weighting strategy that takes into account the sparse nature of the seismic signal and is robust against missed detections and clutter, which could appear in the form of other impulsive sources or other walkers. Based on the target's range from the seismic sensor array, the received signal's wavefront could either be planar or circular. For circular wavefronts, the footfall location in x-y coordinates is observable by an array. However, for planar wavefronts, only bearing (θ) estimates can be made. Our weighting strategy automatically makes use of the wavefront shape and assigns weights to the particles in x-y space. Thus our method is superior to standard beamforming approaches [2] that rely on the assumption that the wavefront is planar. Between consecutive footfalls, the particles are allowed to coast pseudo-randomly. When the next footfall is detected, particles are assigned weights based on the probability that the footfall occurred at the particle location. Our weighting strategy has additional advantages in the case of multiple walkers since data association is built in and explicit association of received impulses with different walkers is not required. This eliminates the need for heuristic methods of data association used in [3]. The weighted particles are then resampled based on their weights, ensuring the survival of those particles that lie in highly probable locations.

Though our algorithm is capable of estimating footfall locations in x-y space, the performance drops as the wavefront gets flatter. Hence good localization is achieved when the footfall occurs close to the array at broadside. As the source location moves further away, range estimates have a large variance. This problem can be mitigated by incorporating a radar sensor that can feed accurate range estimates into the system. The radar measurements can be processed indepen-

Prepared through collaborative participation in the Advanced Sensors Consortium sponsored by the U. S. Army Research Laboratory under the Collaborative Technology Alliance Program, Cooperative Agreement DAAD19-01-02-0008.

IEEE AC paper

dent of the seismic measurements and the output can be used to classify a target as a moving human based on radar cross section and gait [4]. Simulation results will show tracking performance with and without fusion with the radar system.

The paper is organized as follows. Section 2 explains the characterization of the simulated seismic footfall signals. Section 3 gives details on the Monte-Carlo algorithm for tracking mobile personnel, and simulation results are given in Section 4.

2. Signal Characterization

When humans walk, their footfalls generate impulsive seismic signals that propagate through the earth. Seismic signals propagate via body waves (compressional and shear waves) and surface waves (Rayleigh and Love waves). Detailed descriptions of these waves can be found in [5–7]. Rayleigh waves carry the bulk of the energy in the footfall signal (67%) and travel further than body waves since they undergo reduced attenuation (R^{-1} versus R^{-2} for body waves) [8]. Hence Rayleigh waves are the most useful waves for footfall localization and we disregard all other waves.

The seismic footfall signal is simulated as a differentiated Gaussian pulse. It was shown in [9] that the maximum in the Fourier spectrum for a footstep signal lies between 30 Hz and 470 Hz. A simulated seismic signal for a single footfall using a 470 Hz pulse is given in Fig. 1.

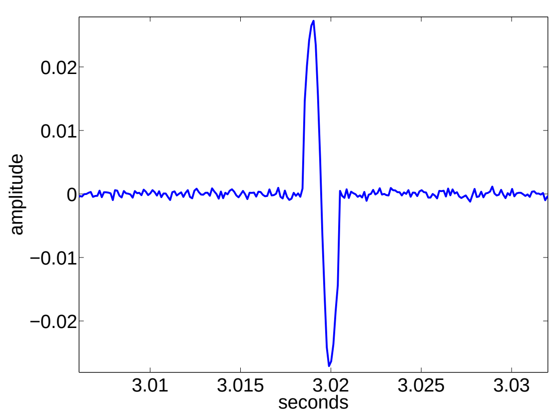

Figure 1. Simulated seismic signal for a single footfall.

A sequence of footfall signals received at a single sensor in the array is given in Fig. 2. Here, the walker is passing by the sensor, so the signal to noise ratio (SNR) varies throughout the signal. The time when the signal strength reaches its maximum value is defined as the closest point of approach (CPA), i.e., the point at which the footfall location is closest to the sensor. At CPA, the SNR of the received signal at a sensor is at its maximum value. As the target moves away from the sensor, the SNR drops inversely to the distance (R) between the footfall location and the sensor. We assume a homogeneous medium of propagation through which Rayleigh waves propagate radially outward from the source at a velocity (v_s) of 2000 m/s and decay inversely with R.

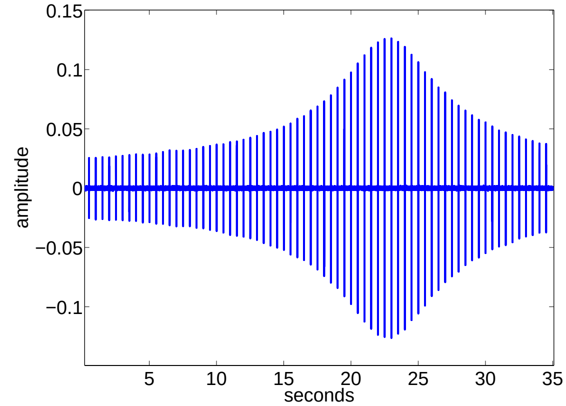

Figure 2. Received footfall signal measured by a seismic sensor.

3. Particle Filter

A particle filter is a sequential Monte-Carlo method used to approximate a posterior distribution of interest, $p\left(\mathbf{s}_t|\mathbf{s}_{t-1},\mathbf{z}_t\right)$, using a weighted set of discrete state realizations called particles. We define the following: $\{\mathbf{s}_t^{(i)}\}_{i=1}^N$ is the set of N particles, $\{w_t^{(i)}\}_{i=1}^N$ is the set of weights associated with the N particles, and $\mathbf{z}_t$ is the measurement vector at time t. The generic particle filter algorithm is given below.

PARTICLE FILTER ALGORITHM

- **STEP 1: Propose Particles**

$$\mathbf{s}_t^{(i)} \sim \pi\left(\mathbf{s}_t|\mathbf{s}_{t-1},\mathbf{z}_t\right)$$

- **STEP 2: Assign Weights**

$$\tilde{w}_t^{(i)} = \frac{p\left(\mathbf{s}_t^{(i)}|\mathbf{s}_{t-1}^{(i)},\mathbf{z}_t\right)}{\pi\left(\mathbf{s}_t^{(i)}|\mathbf{s}_{t-1}^{(i)},\mathbf{z}_t\right)} \propto \frac{p\left(\mathbf{z}_t|\mathbf{s}_t^{(i)}\right)\cdot p\left(\mathbf{s}_t^{(i)}|\mathbf{s}_{t-1}^{(i)}\right)}{\pi\left(\mathbf{s}_t^{(i)}|\mathbf{s}_{t-1}^{(i)},\mathbf{z}_t\right)}$$

$$w_t^{(i)} = \frac{\tilde{w}_t^{(i)}}{\sum_{j=1}^N \tilde{w}_t^{(j)}}$$

- **STEP 3: Resample Particles**

$$\mathbf{s}_t^{(i)} \sim \sum_{j=1}^N w_t^{(j)} \delta\left(\mathbf{s}_t - \mathbf{s}_t^{(j)}\right)$$

■

The standard particle filter algorithm consists of three main steps. In the first step, particles are sampled from an appropriate proposal function, $\pi\left(\mathbf{s}_t|\mathbf{s}_{t-1},\mathbf{z}_t\right)$. In the second step, all the particles are assigned weights, $\{w_t^{(i)}\}_{i=1}^N$, to compensate for the discrepancy between the proposal function used and the posterior distribution we are trying to approximate. In the optional third step, particles are resampled to replicate particles with large weights and eliminate particles with low weights. The resampling step is necessary to avoid degeneracy of the algorithm [10].

Since each sensor provides seismic data continuously, we propose to process the incoming data in segments by using a sliding window. At each iteration of the particle filter, only the data that lies in the current window for each sensor is processed. Windows used at each iteration overlap one another. This must be done to avoid the situation that arises when the signal corresponding to the same footstep appears in the windowed data for different sensors at different times and is processed during different iterations of the particle filter.

For optimal operation, particles should be sampled from the posterior distribution of interest, utilizing knowledge of particles at the previous time as well as current measurements [10]. Since footfalls generate sparse signals, the particle filter iterates at a higher rate than the footfall frequency and information useful to determine footfall locations may not be available at every iteration. Hence, we use a bootstrap approach [11] in which particles are proposed using only the prior distribution

$$\pi\left(\mathbf{s}_t|\mathbf{s}_{t-1},\mathbf{z}_t\right) = p\left(\mathbf{s}_t|\mathbf{s}_{t-1}\right) = N\left(\mathbf{A}\mathbf{s}_{t-1}^{(i)},\Sigma_{\mathbf{s}}\right). \qquad (1)$$

We choose as our state vector $\mathbf{s}_t^{(i)} = [x_t,\ y_t,\ v_{x,t},\ v_{y,t}]^T$, representing the x-y positions and velocities. The system in (1) has been modeled using a locally constant velocity assumption, where $\mathbf{A}$ is the state transition matrix. This allows particles to coast pseudo-randomly when no footfall is present in the received signal, with acceleration entering the system in the form of Gaussian noise with covariance $\Sigma_{\mathbf{s}}$.

For the choice of proposal function in (1), the weighting function is proportional to the data likelihood

$$w_t^{(i)} \propto p\left(\mathbf{z}_t|\mathbf{s}_t^{(i)}\right). \qquad (2)$$

The choice of the weighting function is a critical factor that has a direct effect on tracking performance. A standard TDOA approach like the one given in [3] uses correlation and geometry to estimate the footfall location from the signals received at the different sensors in the array. This method provides poor tracking results when multiple walkers or impulsive sources of noise are present because explicit data association must be performed using heuristic methods. Another problem is that a footfall must first be detected in the signal before performing TDOA analysis. This can be accomplished using a matched filter approach where the received seismic signal at each sensor is matched against a waveform resembling a footstep signal [3] or by calculating kurtosis and cadence [12], both of which increase the computational load and are not very reliable. Standard beamforming approaches [2] rely on the assumption that the received wavefront is planar. These methods work well when the target is at a large range from the sensor but perform poorly when the range is small and the wavefront is circular, which is the case generally encountered considering standard detection ranges for human footfall signals [13].

We choose a novel weighting function in which the data likelihood $p\left(\mathbf{z}_t|\mathbf{s}_t^{(i)}\right)$ is proportional to the power of the combined signal obtained when the envelopes of the seismic signals received by each sensor in the seismic array are shifted in time and added together assuming that the true footfall occurred at the location of particle $\mathbf{s}_t^{(i)}$.

$$\Delta_m^{(i)} = \frac{\sqrt{\left(x_t^{(i)} - x_m\right)^2 + \left(y_t^{(i)} - y_m\right)^2}}{v_s}, \qquad (3)$$

$$p\left(\mathbf{z}_t|\mathbf{s}_t^{(i)}\right) \propto P\left\{\sum_{m=1}^{M}\delta\left(t+\Delta_m^{(i)}\right) * \left(S_m \cdot W(t)\right)\right\}. \quad (4)$$

Here $(x_t^{(i)}, y_t^{(i)})$ represents the x-y location of particle i, (x_m, y_m) represents the x-y location of sensor m, S_m represents the envelope of seismic signal received at sensor m, $W(t)$ is an appropriate windowing function, and $P\{\cdot\}$ returns the power of the argument. The envelope of the seismic signal can be determined by taking the absolute value of the incoming signal, low pass filtering it and removing the DC bias as shown in Fig. 3. Convolution of the windowed signal with the

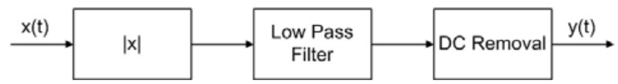

Figure 3. Envelope Detector.

Dirac delta function $\delta(\cdot)$ produces a time shift. Due to dispersion, the raw waveforms received at one sensor may not be correlated with the raw waveforms received at other sensors [3]. In such cases, even if the waveforms received at all sensors in the array were delayed and summed correctly, they still might not add coherently. Therefore, rather than using the true received signal, we use the envelope of the received signal at each sensor.

A similar approach is used in [14] where the signal energy is calculated at predetermined fixed grid locations and the location with the maximum energy is assumed to be the true footfall location. The total number of grid locations depends on the area under observation and the desired resolution for localization. If a high resolution grid is used, then this method requires a large number of computations for accurate localization. To limit the amount of computation, the number of grid locations must be limited to a reasonable amount. If a large area is to be monitored, this method can fail since the location where energy is calculated may not coincide with a footfall location due to lack of resolution. This is the curse of dimensionality. Instead of using a fixed grid, our particle filter algorithm uses an adaptive grid where the grid locations are defined by the particle positions. Our method is superior to [14] since the particle support provides high resolution in areas of interest only, hence reducing the total number of computations required for localization and tracking.

Advantages Over TDOA and Beamforming Methods

Our method has advantages over TDOA methods as well as standard beamforming methods.

- *Calculation of kurtosis is not required.*

The weighting function is applied to each window of incoming data. If no footfall data is present, then the data contains uncorrelated noise and the weights assigned to each particle are almost equal. Thus particles survive the resampling step and are allowed to coast. If a footfall did occur, then only those particles that are located in the vicinity of the true footfall location have high weights. This is because the signals received at the different sensors would add up coherently after processing for those particles only (see Fig. 4.)

- *Explicit data association for multiple targets or clutter is not required.*

The particles located in the vicinity of the true footfall location would have large weights since the signals received at the different sensors would add up coherently after processing for those particles only. Impulsive signals originating at locations different from the particle locations would not add coherently after processing. In this case the weights for all particles would be almost equal, enabling them to survive the resampling step and coast (see Fig. 5).

- *Assumption of a planar wavefront is not required.*

The range and bearing resolution provided by the weighting function vary with the curvature of the wavefront. As the range to the true footfall location increases, the wavefront gets flatter and range resolution is lost. Bearing resolution improves with increase in range but even at close range, bearing resolution is still preserved. This behavior is demonstrated in Figs. 6 and 7 for a linear array. Thus when the footfall occurs at a large distance from the array, only θ estimates can be made and the algorithm performs similar to standard beamforming methods. However, when the footfall occurs close to the array, localization in x-y coordinates is possible.

The accuracy of our algorithm for footfall localization is strongly dependent on two factors: (i) the duration of the signal generated by each footfall and (ii) the range to the footfall location from the sensor array. To demonstrate the effect of duration on localization performance, a Gaussian pulse having a bandwidth of 50 Hz is used to simulate a footfall signal with a longer duration than the signal shown in Fig. 1. The range and bearing resolution plots are given in Fig. 8 for footfalls occurring at broadside. When compared to Figs. 6(a) and 7(a), the plots in Fig. 8 representing the weighting functions are significantly flattened. Hence, localization performance drops as the footfall duration increases.

It can be seen in Fig. 6 that the range resolution drops as the impulsive source moves further away from the array. To mitigate this problem, we can incorporate range estimates using a radar node. The radar node we use is the new low power RF sensor, implemented at the University of Florida, that uses a microwave signal to determine the range, the radial velocity, and the size of detected targets [4]. The sensor is capable of providing range estimates at 32 ms intervals with a range resolution of approximately 2 m on a range-Doppler map. Up to 100 m, the current system is capable of producing range estimates for multiple ground vehicles as well as human targets. The radar hardware is envisioned to have a larger detection range with hemispherical coverage in the future. In our application, we can achieve significant improvements in tracking by incorporating range measurements from the radar.

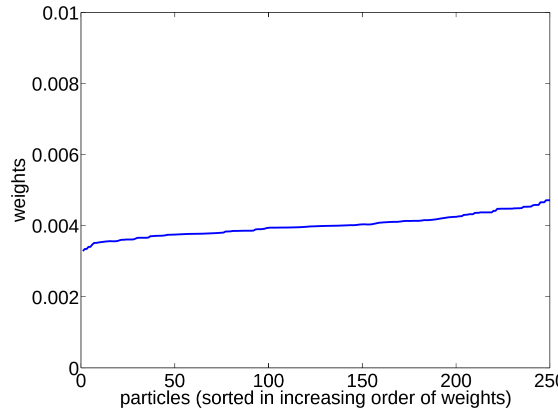

(a)No footfall present.

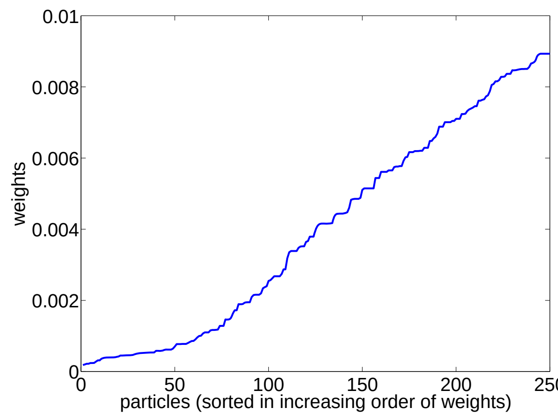

(b)Footfall present.

Figure 4. Comparing weight distribution with and without footfalls present in the windowed data.

The radar measurements and the seismic array measurements can be assumed to be independent given the true footfall location. Hence the joint data likelihood can be factored into the product of the individual data likelihoods.

$$p\left(\mathbf{z}_{s,t}, \mathbf{z}_{r,t}|\mathbf{s}_t^{(i)}\right) \propto p\left(\mathbf{z}_{s,t}|\mathbf{s}_t^{(i)}\right) p\left(\mathbf{z}_{r,t}|\mathbf{s}_t^{(i)}\right), \quad (5)$$

where $\mathbf{z}_{s,t}$ is set of measurements from the seismic array and $\mathbf{z}_{r,t}$ is the set of radar measurements. The data likelihood for the seismic measurements is still (4). A robust likelihood function that accounts for missed detections, clutter and multiple targets is required for the radar measurements.

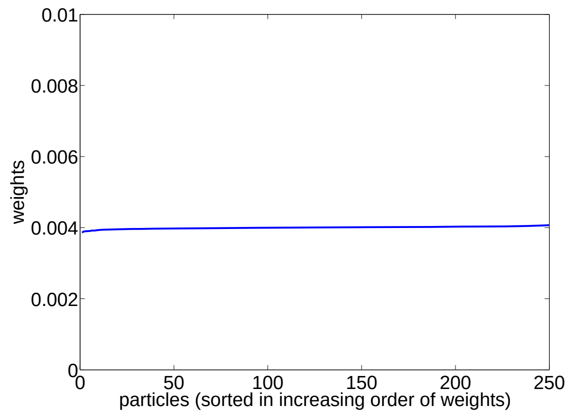

(a)Impulsive signal originating away from the particle support.

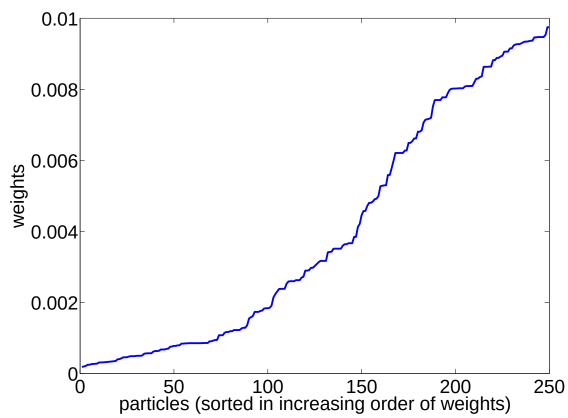

(b)Impulsive signal originating from within the particle support.

Figure 5. Comparing weight distribution when the impulsive signal originates from either within or away from the particle support.

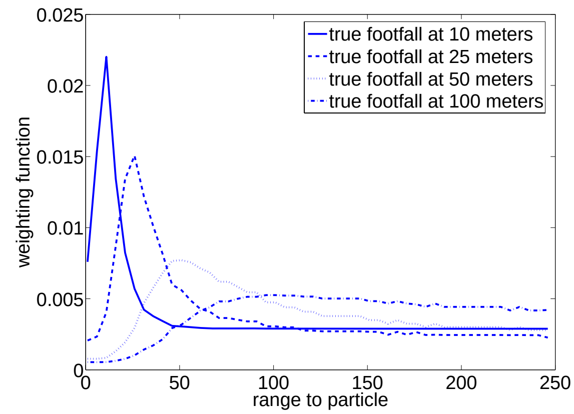

(a)Impulsive signal originating at broadside.

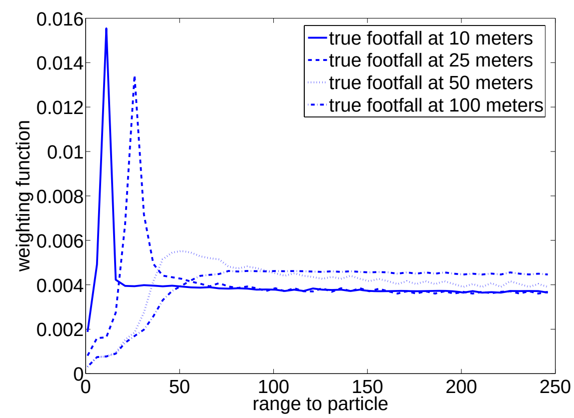

(b)Impulsive signal originating at a 60° angle.

Figure 6. Range resolution decreases as the impulsive source moves away from the array.

The approach used here is similar to the approach used in [15, 16]. Assume that the radar node has K measurements. Then, given a particle $\mathbf{s}_t^{(i)}$, the radar measurements $\mathbf{z}_{r,k,t}$, $k = 1, ..., K$, could have been generated either by a target or by clutter. The clutter distribution is assumed to be Poisson with spatial density λ. The probability of miss is set equal to a constant q. It is assumed that there is an equal probability for each of the K measurements to be a true measurement and the true target measurement is Gaussian distributed about the true target state. Thus, as shown in [15] the likelihood function can be represented as:

$$p\left(\mathbf{z}_{r,t}|\mathbf{s}_t^{(i)}\right) \propto 1+\frac{1-q}{\sqrt{2\pi\sigma^2}q\lambda}\cdot\sum_{k=1}^{K}\exp\left\{\frac{\left(\mathbf{z}_{r,k,t}-r_t^{(i)}\right)^2}{2\sigma}\right\}, \quad (6)$$

where $r_t^{(i)}$ is the distance between particle $\mathbf{s}_t^{(i)}$ and the radar sensor and σ is the standard deviation of the Gaussian distribution used to model the radar measurement error. The final particle weights are proportional to the overall likelihood function (5) which is evaluated by taking the product of the radar likelihood (6) and the seismic likelihood (4).

4. SIMULATIONS

A sensor array consisting of 6 seismic sensors is set up linearly along the x axis with uniform spacing of 10 m between the sensors. Walkers are simulated by setting a path on which footfalls are generated between 2–3 Hz, which is a reasonable gait frequency. Uncorrelated white noise of fixed variance is added to the signal received at each sensor. Since the Rayleigh waves carrying the seismic footfall signal decay as R^{-1}, the received SNR varies at each seismic sensor based on the range to the true footfall location. In all the following simulations, the initial states of the walkers are assumed to be known. 250 weighted particles are used to represent the tracking posterior in all simulations.

For some simulations a radar node is used to improve range resolution. This is particularly helpful when the footfall occurs at a large distance from the seismic array and the wavefront is planar. The radar node is placed at the center of the seismic sensor array. Only the range estimates provided by the radar are fed into the algorithm. The simulated radar sen-

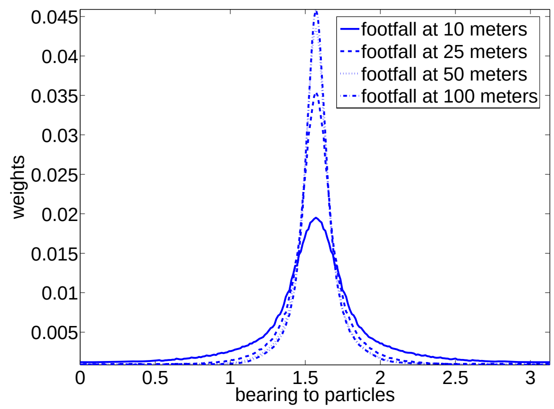

(a)Impulsive signal originating at broadside.

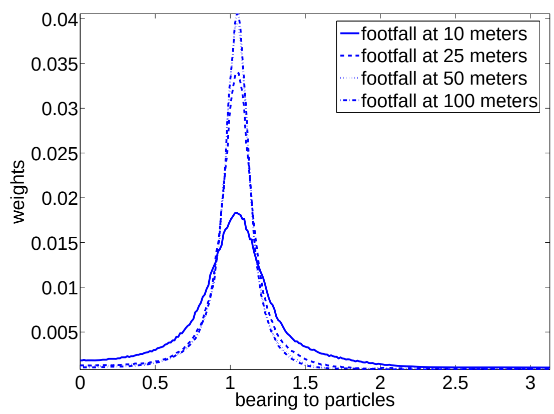

(b)Impulsive signal originating at a 60° angle.

Figure 7. Bearing resolution improves as the impulsive source moves away from the array.

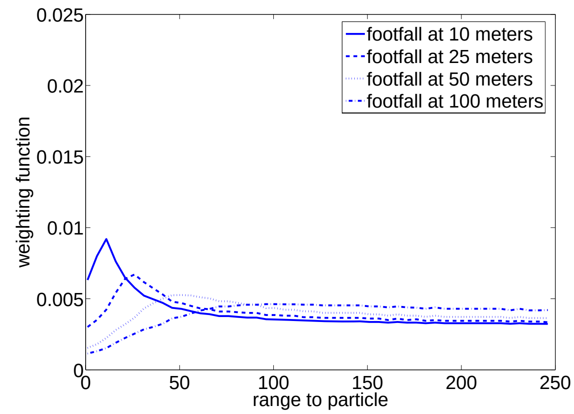

(a)Range resolution.

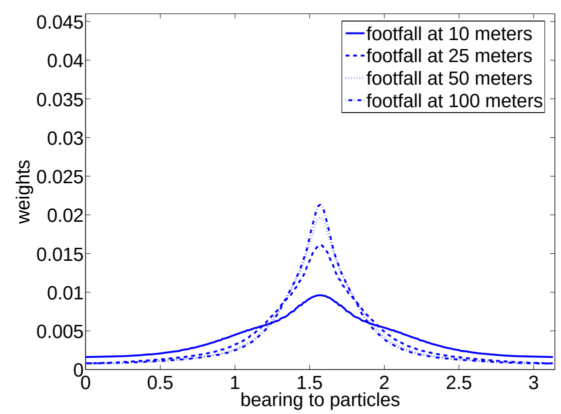

(b)Bearing Resolution.

Figure 8. Range and bearing resolution when the temporal size of the footfall signal is large.

sor has a measurement error with a standard deviation of 2 m. The radar is assumed to have hemispherical coverage and is not capable of observing the target's bearing. Hence bearing tracking is accomplished by the seismic array alone. In all the given plots, the seismic sensor nodes are denoted with a star $*$, and the radar node with ∇. The dotted line represents the true footfall locations, and the solid line the estimated track.

The algorithm is first simulated for a single walker moving in a zigzag path near the linear array. The walker starts at location (-8 m, 13 m) and ends at (54 m, 12 m). The Gaussian pulse used to simulate the footfall signal has a temporal duration of approximately 0.00212 s, which corresponds to approximately 470 Hz. The simulation results are given in Fig. 9. The estimated track is generated using a weighted average of the set of particles. As expected, the track is jittery because not all footfalls are detected during every particle filter iteration. During such iterations, the particles are allowed to coast pseudo-randomly. It is clearly seen that accurate x-y tracking is possible using a small array of seismic sensors.

The same simulation is repeated using longer Gaussian pulses, approximately 0.02 s corresponding to about 50 Hz,

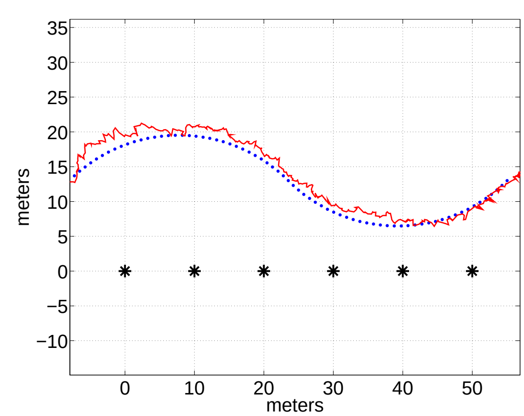

Figure 9. Simulation results for tracking a single walker using only a seismic sensor array. The duration of each footfall signal is short.

to simulate footfalls. Tracking results in Fig. 10 show a significant decrease in performance when compared to Fig. 9. This clearly demonstrates that longer durations of the footfall signal will worsen the tracking performance. The rest of the simulations will focus on the case of short duration footfall signals only.

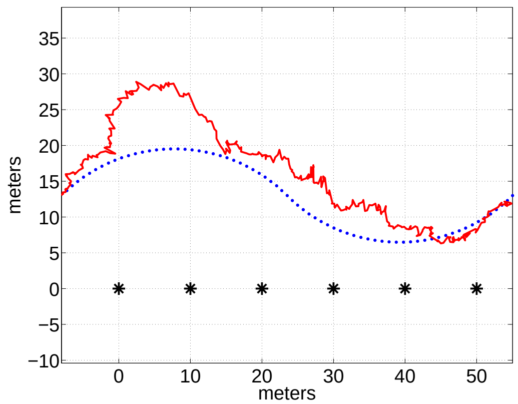

Figure 10. Simulation results for tracking a single walker using only a seismic sensor array. The duration of each footfall signal is long.

Figure 11 shows simulation results for the same walker when the radar node is also used for the case when the footfall signal duration is approximately 0.00212 s. Improvements in tracking results can be seen but they are not very significant since the seismic array does a good job of localizing the footfalls when they occur close to the array.

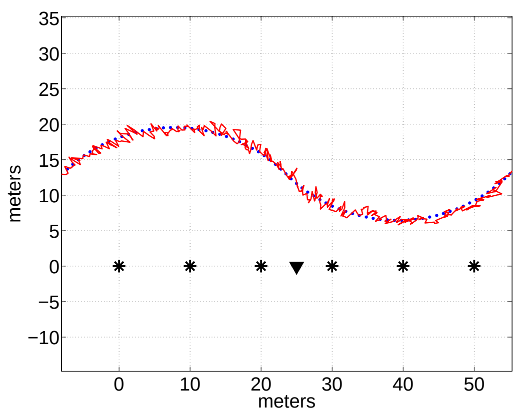

Figure 11. Simulation results for tracking a single walker using a seismic sensor array and a radar node.

The simulation in Fig. 12 shows tracking results for a walker moving along a path similar to the one in the preceding simulations, but at a larger distance from the seismic array. As expected, range resolution is lost and the tracking accuracy reduces when compared to Fig. 9. When the same simulation is repeated using the radar node in addition to the seismic array, tracking results are significantly improved as shown in Fig. 13. In this case, the range resolution provided by the radar node is much higher than the range resolution provided by the seismic array alone. Thus the performance gain with a radar node is much greater when the target is at a larger distance from the sensors.

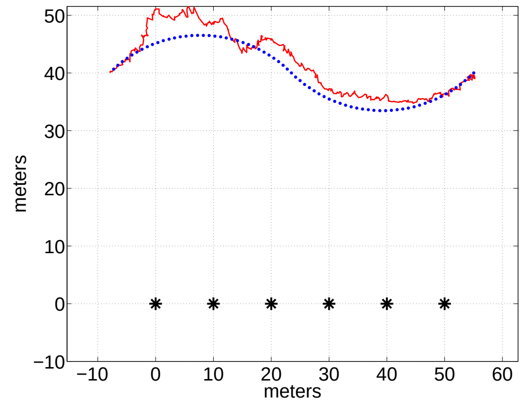

Figure 12. Simulation results for tracking a single walker at a large distance from the seismic sensor array.

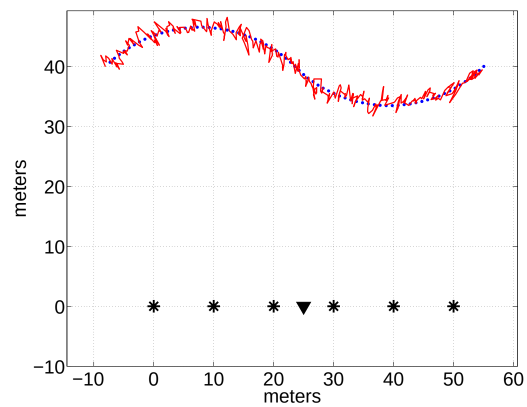

Figure 13. Simulation results for tracking a single walker at a large distance from the seismic sensor array and the radar node.

Simulations for tracking multiple simultaneous walkers are given in Figs. 14 and 15. Figure 14 shows tracking results when only the seismic array is used. Though both walkers are tracked, the tracking accuracy for the distant target is quite poor. When radar measurements are incorporated into the system, tracking results improve significantly (see Fig. 15).

5. Conclusions and Future Work

A novel Monte-Carlo method for tracking multiple walkers using seismic sensor arrays was proposed and simulated. The algorithm can track multiple walkers without explicit data association and is robust against missed detections and clutter. A novel weighting function utilizes the shape of the wavefront and, when the wavefront is circular, can localize impulsive signal sources in x-y space. The algorithm offers advan-

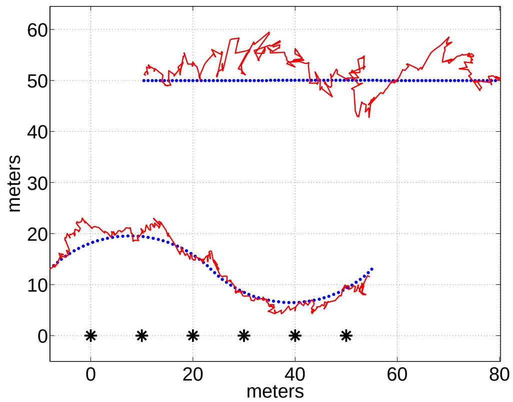

Figure 14. Simulation results for tracking multiple walkers using only a seismic sensor array.

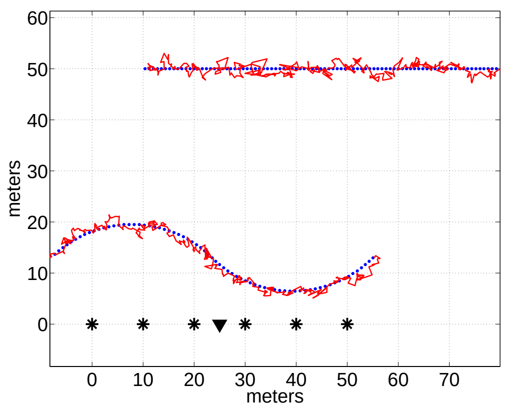

Figure 15. Simulation results for tracking multiple walkers using a seismic sensor array and a radar node.

tages over standard TDOA approaches as well as beamforming approaches. If the wavefront is planar, which is the case when the target is at a large distance from the sensor array, we incorporate range estimates into our system using radar.

Currently the target's motion is modelled by a locally constant velocity assumption. This is not the ideal model for human motion and it fails when the target undergoes sudden movements. Future work will focus on developing hybrid motion models that better approximate human motion.

References

[1] Y.T. Chan and K.C. Ho, "A simple and efficient estimator for hyperbolic location," *IEEE Trans. on Signal Processing*, vol. 42, no. 8, pp. 1905–1915, 1994.

[2] B.D. Van Veen and K.M. Buckley, "Beamforming: a versatile approach to spatial filtering," *IEEE ASSP Magazine*, vol. 5, no. 2, pp. 4–24, 1988.

[3] M. Richman, D. Deadrick, R. Nation, and S. Whitney, "Personnel tracking using seismic sensors," in *Proc. SPIE*, 2001, vol. 4393, pp. 14–21.

[4] J.L. Kurtz and P.R. Carlson, "A radar microsensor for fusion with acoustic, seismic magnetic and imaging sensors," in *Proc. MSS Battlespace Acoustics and Magnetic Sensors Symposium*, 2006.

[5] B.A. Bolt, *Earthquakes and Geological Discovery*, Scientific American Library, 1993.

[6] B.A. Bolt, *Earthquakes*, W. H. Freeman, 2003.

[7] P. Shearer, *Introduction to Seismology*, Cambridge University Press, 1999.

[8] G. Succi, G. Prado, R. Gampert, T. Pedersen, and H. Dhaliwal, "Problems in seismic detection and tracking," in *Proc. SPIE*, 2000, vol. 4040, pp. 165–173.

[9] X. Li, R.J. Logan, and R.E. Pastore, "Perception of acoustic source characteristics: Walking sounds," *J. Acoustical Society of America*, vol. 90, pp. 3036–3049, 1991.

[10] A. Doucet, "On sequential simulation-based methods for Bayesian filtering," Tech. Rep. CUED/F-INFENG/TR.310, Department of Engineering, University of Cambridge, 2001.

[11] N.J. Gordon, D.J. Salmond, and A.F.M. Smith, "Novel approach to nonlinear/non-gaussian bayesian state estimation," in *IEE Proceedings F, Radar and Signal Processing*, 1993.

[12] G. Succi, D. Clapp, R. Gampert, and G. Prado, "Footstep detection and tracking," in *Proc. SPIE*, 2001, vol. 4393, pp. 22–29.

[13] A. Pakhomov, A. Sicignano, M. Sandy, and T. Goldburt, "Seismic footstep signal characterization," in *Proc. SPIE*, 2003, vol. 5071, pp. 297–305.

[14] R. Yong and D. Florencio, "New direct approaches to robust sound source localization," in *Proc. 2003 Intl. Conf. on Multimedia*, 2003, vol. 1, pp. 737–740.

[15] Y. Bar-Shalom and T. Fortmann, *Tracking and Data Association*, Academic-Press, 1988.

[16] M. Isard and A. Blake, "Condensation – conditional density propagation for visual tracking," *International Journal of Computer Vision*, vol. 29, pp. 5–28, 1998.

Milind Borkar *was born in Mumbai, India in 1980. He received his B.S. and M.S. degrees in Electrical and Computer Engineering at the Georgia Institute of Technology in 2002 and 2005 respectively. He was employed by Intel Corporation, Beaverton, Oregon and Texas Instruments, Dalls, Texas in 2001 and 2006 respectively. He is currently a Ph.D. student in Electrical Engineering under the supervision of Dr. James H. McClellan. His research interests include Markov chain Monte-Carlo methods, smart sensor networks, heterogeneous sensor fusion, personnel detection and tracking, and development of multimedia tools for education.*

Volkan Cevher *was born in Ankara, Turkey, in 1978. He received his B.S. degree in Electrical Engineering from Bilkent University, Ankara, Turkey in 1999 as a valedictorian. During the summer of 2003, he was employed by Schlumberger Doll Research. In Fall 2004, he was the co-recipient of the Center for Signal and Image Processing Outstanding Research Award. He received his Ph.D. degree in Electrical Engineering from Georgia Institute of Technology in 2005. He worked as a post-doc at Georgia Institute of Technology under the supervision of Dr. James H. McClellan till the end of 2005. He is currently working with Dr. Rama Chellappa as a research associate on computer vision problems. His research interests include structure from motion, sensor network management problems (sensor build and placement strategies), Monte-Carlo Markov chain methods (specifically particle filters), target tracking models, adaptive filters, time frequency distributions, fractional Fourier transform, and array signal processing.*

James H. McClellan *received the B.S. degree in Electrical Engineering from L.S.U. in 1969, and the M.S. and Ph.D. degrees from Rice University in 1972 and 1973, respectively. From 1973 to 1982, he was a member of the research staff at Lincoln Laboratory and then a professor at MIT. From 1982 to 1987, Dr. McClellan was employed by Schlumberger Well Services. Since 1987, he has been a Professor in the School of Electrical and Computer Engineering at Georgia Tech, where he presently holds the John and Marilu McCarty Chair.*

He is a co-author of the texts Number Theory in Digital Signal Processing, Computer Exercises for Signal Processing, DSP First: A Multimedia Approach, *and* Signal Processing First, *which received the McGraw-Hill Jacob Millman award for an innovative textbook in 2003. In 1998, Prof. McClellan received the W. Howard Ector Outstanding Teacher Award at Georgia Tech, and in 2001, the Education Award from the IEEE Signal Processing Society. In 1987, he received the Technical Achievement Award for work on FIR filter design, and in 1996, the Society Award, both from the IEEE Signal Processing Society. In 2004, he was a co-recipient of the IEEE Kilby medal. Prof. McClellan is a Fellow of the IEEE and a member of Tau Beta Pi and Eta Kappa Nu.*